# Supplementary Materials for

## Clinically relevant mutations in core metabolic genes confer antibiotic resistance

Allison J. Lopatkin, Sarah C. Bening, Abigail L. Manson, Jonathan M. Stokes, Michael A. Kohanski, Ahmed H. Badran, Ashlee M. Earl, Nicole J. Cheney, Jason H. Yang, James J. Collins*

*Corresponding author. Email: jimjc@mit.edu

Published 19 February 2021, *Science* **371**, eaba0862 (2021)
DOI: 10.1126/science.aba0862

**This PDF file includes:**

Materials and Methods
Figs. S1 to S11
Tables S1 and S2
Captions for Tables S3 to S15
References

**Other Supplementary Material for this manuscript includes the following:**
(available at science.sciencemag.org/content/371/6531/eaba0862/suppl/DC1)

Tables S3 to S15 (Excel files)
MDAR Reproducibility Checklist (PDF)

## Materials and Methods

Mathematical modeling

To estimate the likely frequencies of metabolic mutations in a classical evolution setup, we adapted a mathematical model previously published (*20*), which calculates the probability that a given mutation will become established in a population over multiple generations, following antibiotic treatment ($P_E$): $P_E = \sum_{t=0}^{T-1} \mu N_0 2^t \left[1 - (1 - S_R)^{2^{T-t}}\right]$. Here, $P_E$ is analogous to mutation frequency in our experiments (i.e., if $P_E = 1$, the mutation is fixed, and the frequency is 100%). $N_0 2^t$ is the size of the population at generation *t*, T is the total number of generations, $S_R$ is the survival rate of each mutation, and μ is the probability for a mutation to occur, which is proportional to the number of genes related to that phenotype. Since there are many more genes involved in metabolism than those related to a specific drug target, the probability of acquiring (i.e., establishing) a metabolism-related mutation is higher; for example, Levin-Reisman et al. showed the probability of acquiring a mutation conferring antibiotic tolerance is higher than that of one conferring resistance, since there are more genes that affect tolerance (e.g., metabolism, toxin/antitoxin systems, etc.) (*20*). In the context of this model, a relatively high value of μ corresponds to a metabolic mutation, whereas a low value of μ corresponds to a mechanism-specific mutation. Moreover, since metabolic mutations have a much broader range of potential effects on the cell, the probability that any individual metabolic mutation increases the overall fitness of a cell is smaller. In other words, mutations that confer a specific phenotypic advantage with the smallest overall effect on the cell's fitness are most likely to be favored (*44–46*). Thus, to model the relative frequency of metabolic mutations, we assume that $S_R$ is inversely proportional to μ (i.e., mutations in canonical genes occur infrequently but have higher probabilities of fixation): $S_R = \frac{K^n}{K^n + \mu^n}$, where K is the mutation rate corresponding to a survival probability of 50%, and n is the Hill coefficient. We set $K = 10^{-14}$ to reflect the overall low likelihood of mutation establishment, and *n*=2. We note that the choice of Hill coefficient did not change simulation results. Moreover, we implemented Gaussian noise (with a coefficient of variance of 5%) to simulate heterogeneous populations. Mutation occurrence and survival were simulated for 60 generations; this was long enough to reveal the relationship between mutation frequency and establishment, whereas excessively long simulations would result in establishment regardless of frequency. Finally, we assumed that μ is independent of antibiotic concentration. This code is archived on Zenodo (*43*).

Classic evolution

The *Escherichia coli* strain BW25113 was used for all experiments. A single colony was picked from a streaked agar plate, and grown in 3 mL MOPS EZ (Teknova, #M2105) rich media overnight shaking at 250 rpm. After 16 hours, triplicates of this clone were saved in 50% glycerol and stored at -80°C for subsequent sequencing and experiments. Cells were diluted 500X into fresh MOPS EZ rich media and aliquoted into one row (12 wells) of a 96-well plate. An additional row of blank MOPS EZ rich media was included immediately below as a contamination control. Cells were sealed with an AeraSeal film (Sigma, #A9224), covered with a fitted plastic cover, and grown for 24 hours shaking at 450 rpm and 37°C. Following the first cycle of pre-growth, cells were diluted 500X into fresh MOPS EZ rich media daily. Antibiotic

was added to all treatment wells, and sterile water was added to the control, at concentrations according to Table S2. All antibiotics were pre-diluted into stocks of 10X at the beginning of the experiment, and stored at -20°C throughout. $OD_{600}$ measurements were taken daily immediately prior to the 500X dilution. Since decreases in $OD_{600}$ were observed beginning on day five, samples were saved daily starting on that day and for every day thereafter, until day 10. Populations were revived by thawing the tops of frozen samples, and diluting 1000X into 1.5 mL fresh MOPS EZ rich media in a deep 96-well plate, such that the top row corresponded to the populations saved on day 5 and the bottom row corresponded to the populations saved on day 10. $OD_{600}$ measurements were taken the following morning to determine the terminal population (Fig. 1C). Cells from each terminal population were streaked directly onto blank agar to acquire individual clones. 1 mL of this overnight culture was pelleted, and frozen at -80°C for 48 hours, to be used directly for genomic extraction (see details below). The remaining volume was aliquoted into volumes of 50 μL and saved in glycerol at -80°C in a final concentration of 25%. Population aliquots were partially thawed for subsequent experiments. Individual clones were picked from agar and grown at 37°C overnight, similarly aliquoted, and genomic DNA was extracted immediately. We note that blank media control wells were included for every day of the evolution, and no contamination was observed.

Metabolic evolution

The identical wild-type BW25113 *E. coli* clone as in the classic evolution was used as the starter strain for these experiments. As with the classic evolution protocol, cells were diluted 500X into either MOPS EZ rich media, or MOPS minimal media supplemented with 0.04% glucose, and aliquoted into one row (12 wells) of a 96-well plate. An additional row of blank media was included immediately below. Cells were sealed with an AeraSeal film, covered with a fitted plastic cover, and grown for 24 hours shaking at 450 rpm and 37°C. Following the first cycle of pre-growth, cells were diluted 500X into fresh respective media; immediately following this dilution, cells were equilibrated to the daily temperature for 30 minutes, followed by one hour of drug treatment. As an example, on day 0, freshly diluted cells were equilibrated to 20°C for 30 minutes, after which they were treated with 40X $MIC_{50}$ at the same temperature for exactly one hour. This concentration corresponds to the concentration reached on day 10 of the classic evolution protocol. Following one hour of treatment, cells were washed 2X with PBS, resuspended in the corresponding media, sealed as with previously, and grown at 37°C for the remaining 22 hours with 450 rpm agitation. Every day thereafter, the equilibration/treatment temperature increased in one-degree increments until day 10, which ended at 30°C. Prior to the dilution every morning, $OD_{600}$ measurements were obtained to track density over the course of the evolution. As with previously, a control row of blank media was included for every day of the experiment, and no cell growth was observed throughout the evolution. The static metabolic evolution was performed identically to the first metabolic evolution, with the following changes: only MOPS minimal media was used to control for growth, and during every antibiotic treatment window, the temperature was maintained at 20°C. Otherwise, the protocol remained identical.

MIC and growth rate measurements

Prior to both evolutions, MIC values were determined according to the following protocol: an overnight WT culture (16 hours at 37°C with agitation at 250 rpm) was diluted 10,000X into MOPS EZ rich media, or MOPS minimal media supplemented with 0.04% glucose, and aliquoted into wells of a 96-well plate. The antibiotics strep, cipro, and carb, were diluted in a separate 96-well plate such that the highest final concentrations would be 50, 1, and 100 μg/mL, respectively, and serially diluted in fold-steps of two for 12 concentrations. Plates were sealed and grown for 24 hours as described above, after which the $OD_{600}$ was taken. All MICs were performed in biological triplicate. Once all replicates were obtained, a Hill curve was fit to the

average data as a function of the antibiotic (Fig. S1), and the half-maximal concentration was taken as the $MIC_{50}$. The lowest concentration at which no increase in $OD_{600}$ was observed was taken as the true MIC. Following the evolution, all MIC measurements were obtained similarly, with the following exceptions: for population-level measurements, cells were diluted 500X from the overnight culture, as this was the cell density at which the evolution was performed, and ensures consistency between replicates. To enable fair comparisons between population and clonal samples, clonal isolates were also diluted 500X. Finally, instead of two-fold dilution steps, antibiotics were diluted in a gradient consistent with the daily evolution protocol (e.g., 85% with the highest concentration at 40X $MIC_{50}$. As with MICs, for all population growth rate experiments, overnight cultures were initiated with 500X thawed glycerol samples. For clonal measurements, single colonies were picked from streaked agar and grown analogously. In all cases, cells were diluted 500X into fresh media, and aliquoted into a 96-well plate at a final volume of 200 μL. When applicable, antibiotic was added at this time. Wells were sealed with 50 μL mineral oil (Sigma, #M5904) and read in a pre-warmed 37°C BioRad plate reader with measurements taken at intervals of 15 minutes. Growth rates were quantified using a method established previously (*47*, *48*). Single colony growth rates were obtained using a method analogous to ScanLag whereby overnight cells were diluted and spread onto pre-warmed agar plates, and placed upside down on an EPSON translucent-imaging scanner located inside a 37°C warm room. Images were obtained once every five minutes, and all images were processed using a custom script in MATLAB. Untreated controls were included in every experiment to account for variability in the time between bringing cells into the warm room, and initiation of image collection.

One-hour survival protocol

Conditions analogous to treatment during the metabolic evolution were implemented for consistency; namely, overnight cultures of cells were diluted 500X, and equilibrated to the described temperature for 30 minutes. Following this, 40X $MIC_{50}$ antibiotic was added to each well, and cells were incubated at the described temperature for exactly one hour. Following treatment, cells were washed 2X in PBS, and CFU was obtained by spot plating immediately thereafter.

gDNA extraction, library prep, high-throughput sequencing, and variant calling

Populations were partially thawed, and to ensure consistency across population samples, equivalent volumes from each well-mixed condition were grown overnight in MOPS EZ rich media (1,000X) in 1.5 mL volume. These overnight population cultures were first streaked onto blank agar to obtain individual colonies for subsequent gDNA extraction. Next, 500 μL of each sample was saved as described previously. Finally, the remaining 1 mL was pelleted and saved for gDNA extraction at -80°C for 48 hours. In that time, clonal plates were grown at 37°C for 16 hours; all colonies were picked and grown as described previously. gDNA from individual clones, populations, and the WT strain was extracted using the PureLink Pro 96 Genomic DNA Kit (# K182104). Pooled libraries were prepared using the plexWell 384 kit supplied from SeqWell; whole-genome sequencing was performed on a HiSeq 2500 Rapid Run flow cell with 150 base paired-end reads with an average read depth of 100X at the Broad Institute. Illumina reads were aligned to the *E. coli* reference strain BW25113 (NCBI Genbank accession CP009273) using BWA version 0.7.17(*49*). Pilon(*28*) version 1.23 was used to call variants occurring with a minimum frequency of 2%; this was performed using the --vcfqe option to obtain quality-weighted read depths according to methods established previously to identify low-frequency mutations(*50*). Additionally, we required SNPs to be supported by a minimum of five reads. Finally, to remove sequencing errors associated with strand bias, SNPs were further filtered

from positions where <33% of the reads for the alternate allele were from either the forward or reverse strand.

Gene ontology (GO) enrichment

Gene lists from the classic and metabolic evolutions were individually analyzed using either EcoCyc or the Princeton GO term finder(*51*). For Figure 3, GO enrichment analysis was performed for biological processes, and P-values were obtained using the Fisher exact test. All genes that overlapped with those identified in the non-treated adapted controls, and >80% of these genes occurred in the control samples, were excluded. Genes from the classical evolution were only enriched in eight categories. Since the last two categories were similar to the sixth category, only the top six categories were included from both evolutions in Fig. 3B-C. The entire list of GO classifications, along with the gene lists used for enrichment, can be found in Table S8.

Comparative analysis of variants to published E. coli genomes

All *E. coli* genomes with L50 < 20 were downloaded from the NCBI Pathogens database (https://www.ncbi.nlm.nih.gov/pathogens/) on 2/21/2018 and uniformly annotated using the Broad Institute's Prokaryotic Annotation Pipeline as in Cerqueira et al. (2017)(*52*). Genomes with classifications of either "clinical" (n=3700) or "environmental" (n=3543) were searched for all coding SNPs identified in our sequencing experiments. For each of the >7000 genomes, Blast was used to identify the top gene hit for each BW25113 gene. If the BLAST e-value was $1x10^{-10}$ or less, and the query genome had a coverage of at least 90%, the ortholog sequence was extracted and multiple alignment was performed using Muscle(*53*). Mutated positions in all genomes in the database that aligned with the BW25113 SNPs were tabulated. Mutations that did not appear at least once in the entire pathogen database were removed from consideration; P-values for over-representation in clinical strains were calculated using Fisher's exact test for all remaining mutations and corrected using the false discovery rate method.

Mutation validation

The plasmid backbone used for all constructs is pAB; this plasmid consists of a strong constitutive synthetic promoter proD, chloramphenicol resistance, and a p15A origin of replication. The control plasmid, pAB191, contains the innocuous gene *lacZ* under the control of proD. All WT genes were obtained from the *E. coli* genome using PCR, and cloned into the pAB backbone using either Gibson assembly or USER cloning. All mutant variants were generated with USER cloning. All final constructs were fully sequenced for validation. The corresponding knockout strains for each relevant gene were obtained from the Keio collection. Each strain was validated using PCR, and kanamycin resistance ($kan^R$) was removed with FLP recombinase (pCP20). All plasmids expressing either the WT or mutant variants were introduced into the strain with the corresponding gene chromosomally deleted, except for *gyrA*, which was introduced into the WT strain BW25113 since this gene is essential. Also, there was no mutant variant for *ycgG*; since the mutation from our study was a large deletion, the knockout strain carrying pAB191 served as the appropriate control. Table S1 provides a complete list of strains and plasmids used in this study, along with primer sequences. All experiments that utilized these strains were conducted in the presence of 100 μg/mL chloramphenicol. All MICs were performed identically as described above. In testing drug susceptibility, we found that resistance to the control gene *ompF* was readily visibly by 10 hours, but not by 24 hours, likely due to mutation from the overexpressed gene. Thus, to test drug susceptibility for all constructs, MIC measurements were taken after 10 hours instead of 24 hours to reduce the likelihood of false resistance due to mutation. At least two biological replicates were obtained for each construct. MICs were determined based on the lowest concentration at which no growth was observed above the background $OD_{600}$. We note that some mutants grew slightly slower than the WT control, including $sucA^M$, as evidenced in Fig. S8. In these cases, MICs were verified by allowing

populations to reach equivalent $OD_{600}$ levels to the control to ensure MICs were comparable; doing so did not change the calculated MIC value at 10 hours for any mutant.

Oxygen consumption rate (OCR), $NAD^+$/NADH ratio and ATP levels

OCR was measured using the Agilent Seahorse $XF^e96$ as previously described. Briefly, Seahorse XF Cell Culture microplates (Agilent, #101085-004) were pre-coated with 100 ng/mL poly-D-lysine (Sigma, #P6407). WT and $sucA^M$ strains were grown overnight in MOPS EZ rich media supplemented with 100 μg/mL chloramphenicol. Cells were diluted 100X into fresh MOPS and grown until they reached an $OD_{600}$ of approximately 0.1. Cells were then back-diluted to $OD_{600}$ = 0.005 and 200 μL diluted cells were dispensed to each well of the coated XF microplates. Three OCR measurements were made at 5 min intervals with 2.5 min measurements and 2.5 min mixing. All samples were randomized on the plate to avoid any systematic biases due to Seahorse measurements. For metabolite measurements, strains were grown overnight as described previously. After 16 hours, cells were diluted 500X in MOPS EZ rich media and treated with each drug, or control, at $MIC_{50}$ concentrations. $NAD^+$/NADH (Promega #G9071) measurements were made using the NAD/NADH-Glo Promega assay in biological triplicate after 30 minutes of treatment. ATP measurements were obtained using the BacTiter-Glo (Promega #G8230) microbial viability assay on overnight cells grown in MOPS EZ rich media.

Fluctuation test

Mutation rates were measured using the well-established fluctuation test in response to rifampicin (rif) (Sigma, #3501) as described previously(*54*). Briefly, concentrations of strep, carb, and cipro were chosen based on the highest concentration that still allowed recovery after 24 hours. Strains were grown overnight as described previously, and diluted 10,000X into 50 mL MOPS EZ rich supplemented with 100 μg/mL chloramphenicol. After 3.5 hours, cells were diluted 1:3 into fresh media containing no drug, or one of the three drugs at the specified concentration. Each condition was split into 10 1-mL aliquots in 14 mL culture tubes and grown for 24 hours at 37°C. Cells were then plated on either LB agar or agar containing 50 μg/mL rif. The likelihood of mutations was calculated on a per plate basis as previously described, using the MSS maximum-likelihood method (*55*). The mutation rate was then determined by normalizing the mutation events per rif plate by the total number of bacteria observed on corresponding drug-free LB agar plates. Statistics were calculated as previously described (*55*) and the error bars indicate 95% confidence intervals.

RNA sequencing and analysis

Strains were grown overnight as previously described. After 16 hours, all strains were diluted identically as in the $NAD^+$/NADH and OCR protocol, namely, 500X into MOPS EZ rich media. Cells were treated with $MIC_{50}$ concentrations of the control strain, and incubated at 37°C with 250 rpm agitation for one hour. Following one hour, cells were flash-frozen, and submitted to Medgenomics for RNA extraction and sequencing. RNA sequencing was performed using NovaSeq 150 base paired end reads with 25M total reads/sample. For analysis, raw sequencing files were downloaded, trimmed using Trimmomatic (*56*), and the quality was verified using FastQC. Next, trimmed sequences were aligned to the same BW25113 genome as above using Star (*57*). Gene counts of aligned reads were quantified using FeatureCounts (*58*), and differential gene expression was performed with edgeR (*59*). Differentially expressed genes were defined as a corrected P-value of $< 0.05$, and a log-2 fold change of $>1$ or $<-1$ for up and down regulation, respectively. All raw sequencing data, differential expression data, and GO enrichment can be found in Tables S12-14.

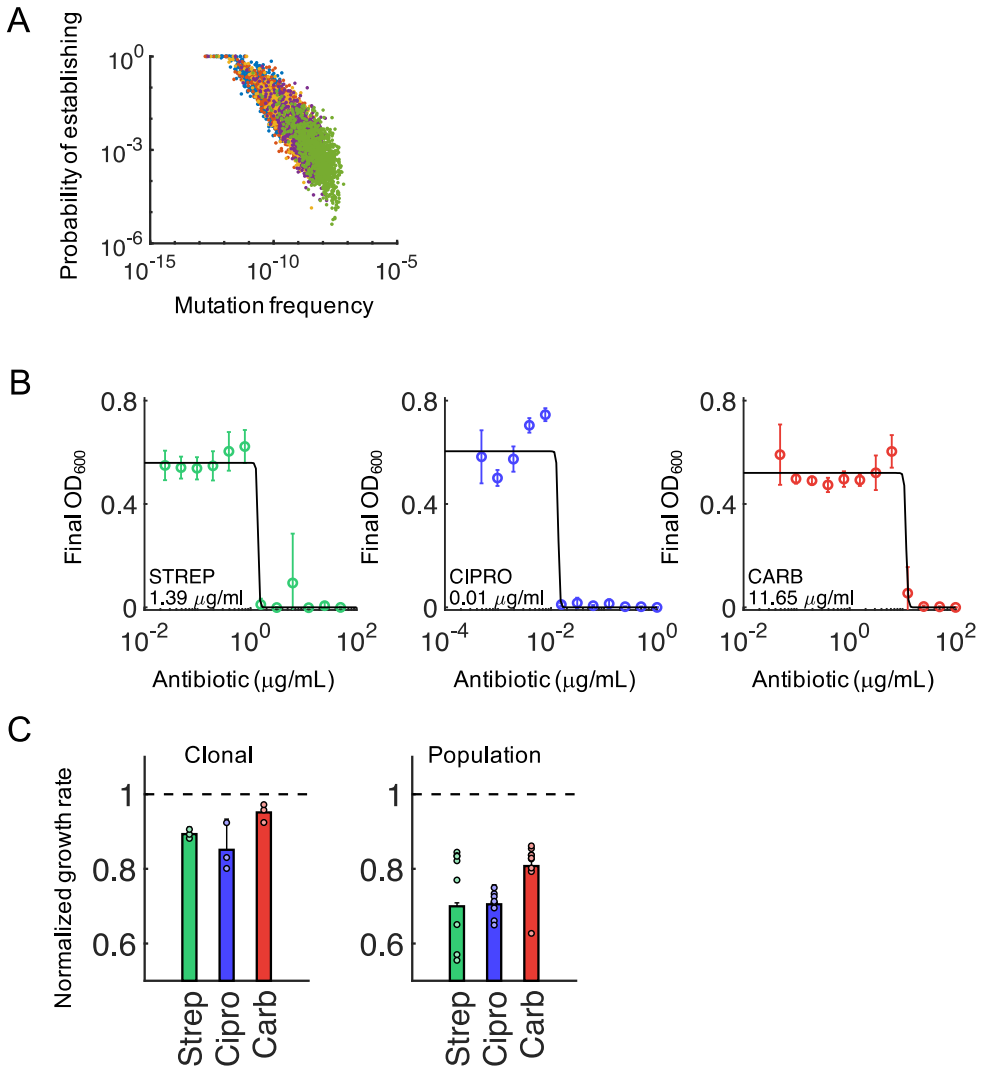


**Fig. S1. Characterization of the classic evolution protocol.**

**(A)** Population genomics model of establishing a metabolic mutation. X-axis is mutation frequency (μ); high μ simulates mutations in metabolic genes, whereas low μ implies a drug target mutation. Colors of blue, orange, yellow, purple, and yellow indicate increasing average μ. **(B)** Calculating the $MIC_{50}$. WT BW25113 was diluted 10,000X into MOPS EZ rich media and grown in the presence of antibiotics at a range of concentrations. After 24 hours, the $OD_{600}$ was taken and the dose response was calculated according to previously established methods. The half-maximal concentration was taken as the $MIC_{50}$. **(C)** Growth rates of 12 individual clones (*left*) or whole populations (*right*) were measured according to previous methods. Growth rates were normalized to the average growth rate of the WT strain, represented by the dashed black line for reference. Bars represent the average of either 12 clones (*left*) or three biological replicates (*right*), and error bars indicate standard deviation.

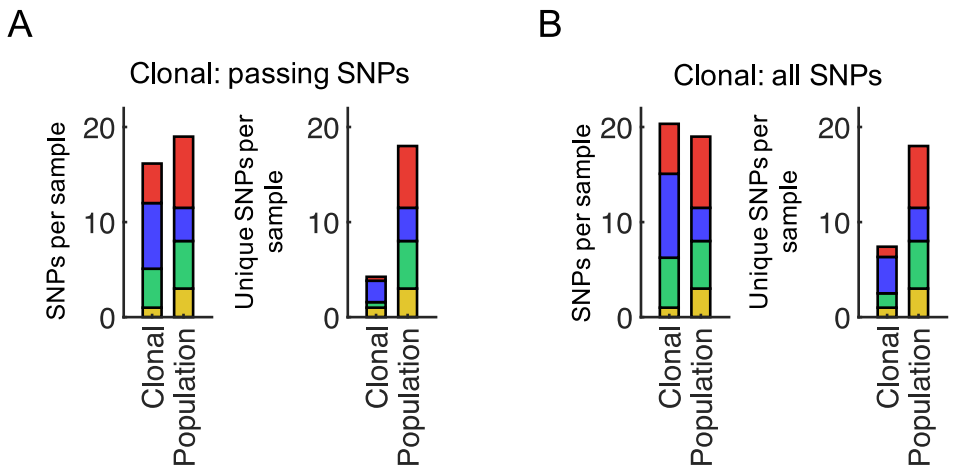


**Fig. S2. Validation for clonal and population SNP detection.**

The finding that unique SNPs per sample is greater in whole population samples than clonal samples was maintained regardless of whether SNPs in the control samples **(A)** or in the clonal samples at frequencies less than passing **(B)** were included.

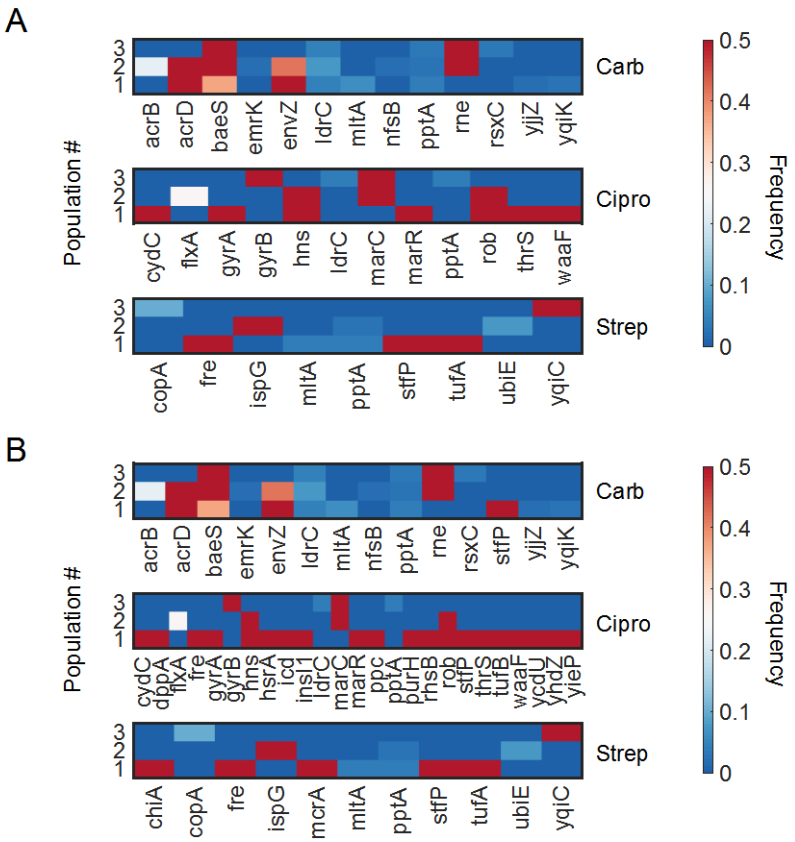


**Fig. S3. SNPs detected in classic evolution.**

Heat maps show variants and their corresponding frequencies that were detected in whole population samples **(A)** or whole populations and passing clonal SNPs **(B)** for each drug. Shading from blue to red represents low to high frequency. For visualization of lower frequency mutants, the frequency scale is set to a maximum of 0.5.

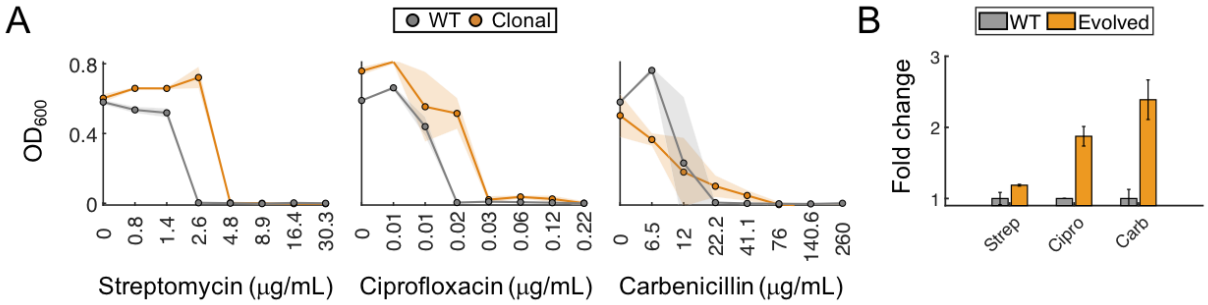


**Fig. S4. MICs from metabolic evolution.**

**(A)** Population-level MICs from whole population samples at the end of the metabolic evolution (orange) compared to the WT strain (gray). To ensure consistency, all population-level measurements were initiated with a 500X dilution from the overnight culture, and grown for 24 hours in MOPS EZ rich media. Following 24 hours, $OD_{600}$ was obtained. The lowest concentration at which no growth occurred was determined as the MIC. Dark lines represent the average of three biological replicates, and shading represents the standard deviation. **(B)** MIC for clones from the metabolic evolution under minimal media. Terminal populations were streaked onto blank agar; 20 clones were picked for the WT strain, and 96 clones were picked for each drug-treated condition. As previously, $OD_{600}$ was measured after 24 hours. The lowest concentration at which no growth occurred was determined as the MIC. Bars represent the average of all clones, and error bars represent standard deviation.

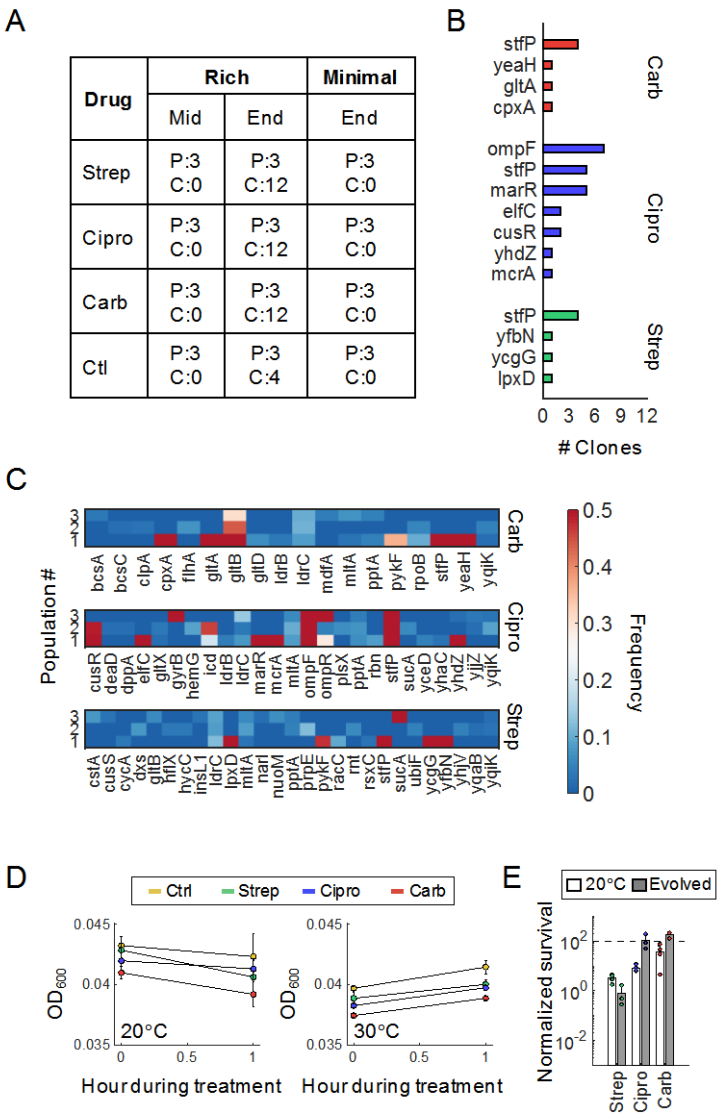


**Fig. S5. Metabolic evolution sequencing results.**

**(A)** Sequencing overview of the metabolic evolution. 12 clones for each treatment condition from the rich media were sequenced, except for the control in which four clones were sequenced. All three terminal populations from both the rich and minimal media from each treatment condition were also sequenced. P stands for population and C for clonal. **(B)** Passing SNPs in sequenced clones. Green, blue, and red bar colors correspond to strep, cipro, and carb, respectively. **(C)** Heat maps of variants and their corresponding frequencies that were detected in whole populations and passing clonal samples for each drug. Shading from blue to red represents low to high frequency. For visualization of lower frequency mutants, the frequency scale is set to a maximum of 0.5. **(D)** Change in $OD_{600}$ before and after 1-hr treatment on day 0 (20°C) and day 10 (30°C). **(E)** Survival for WT cells at 20°C. Evolved cells at 30°C is shown as comparison (same as in Fig. 2D).

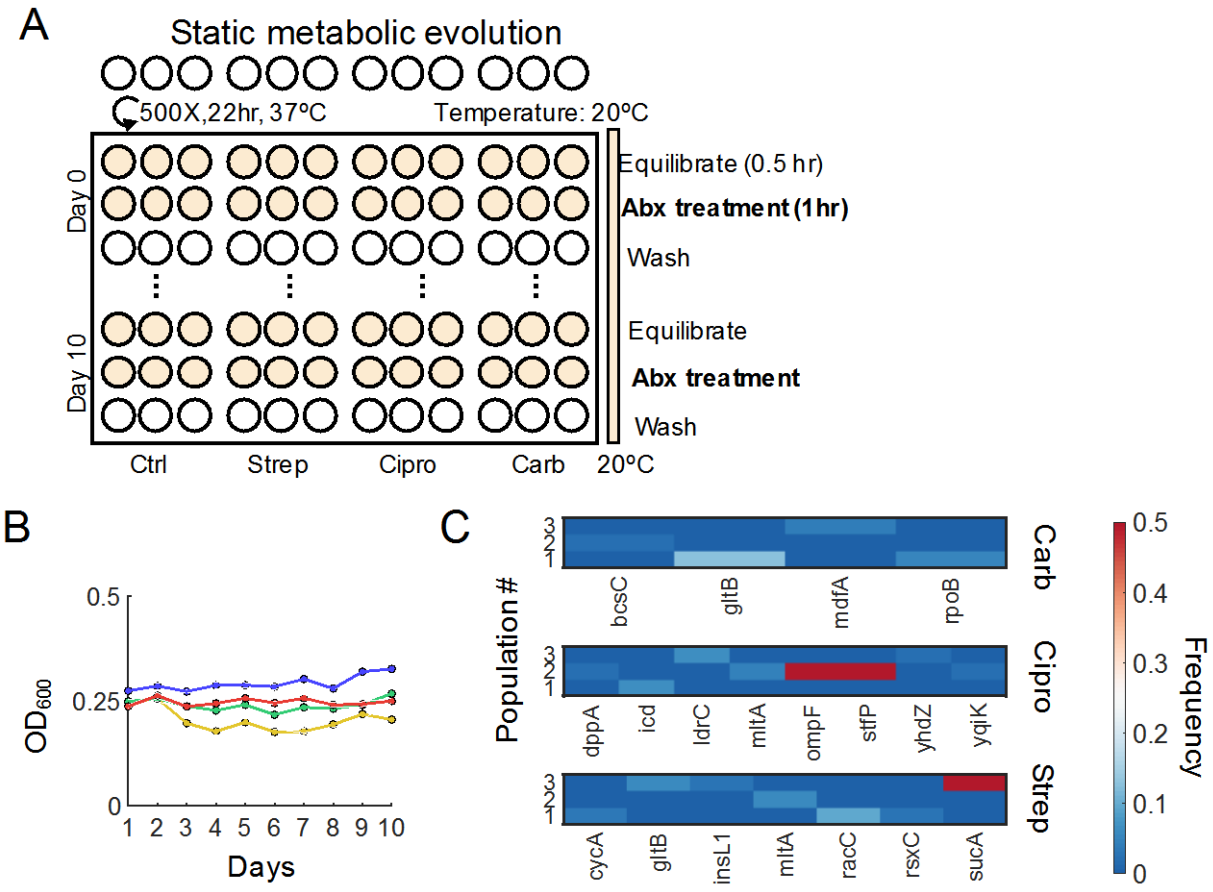


**Fig. S6. Static metabolic evolution.**

**(A)** Evolution schematic. The protocol is identical to the increasing metabolic evolution, except that the temperature is maintained at 20°C every day during the 1-hr treatment for each condition. **(B)** Daily $OD_{600}$ measurements. Shaded color represents standard deviation of three population replicates. Colors yellow, green, blue, and red indicate control, strep, cipro, and carb, respectively. (**C)** Heat maps of variants and their corresponding frequencies that were detected in whole populations for each drug. No clonal isolates were sequenced. Shading from blue to red represents low to high frequency. For visualization of lower frequency mutants, the frequency scale is set to a maximum of 0.5.

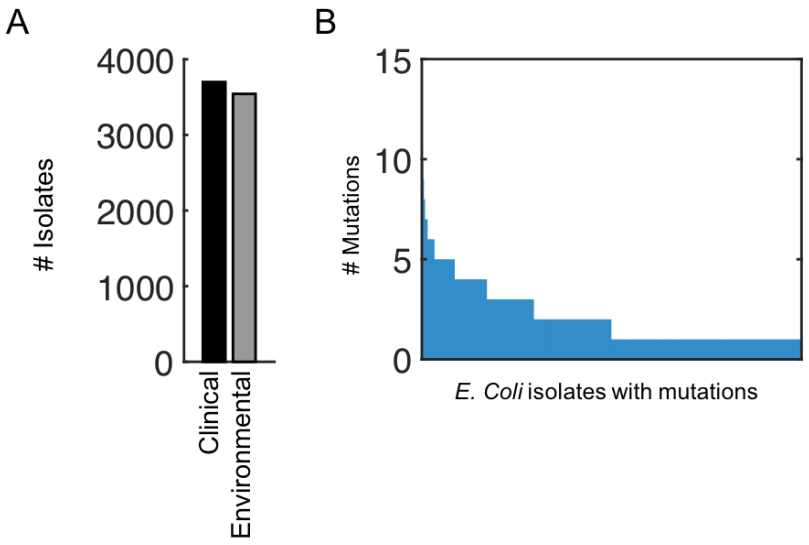


**Fig. S7. Number of mutations per *E. coli* genome.**

**(A)** Total number of NCBI *E. coli* isolates broken down by those designated as "clinical" and those designated as "environmental". **(B)** All NCBI *E. coli* isolates that had at least one mutation identical to one from this study are plotted against the total number of mutations identified in that genome. Each pathogen had less than 10 SNPs each.

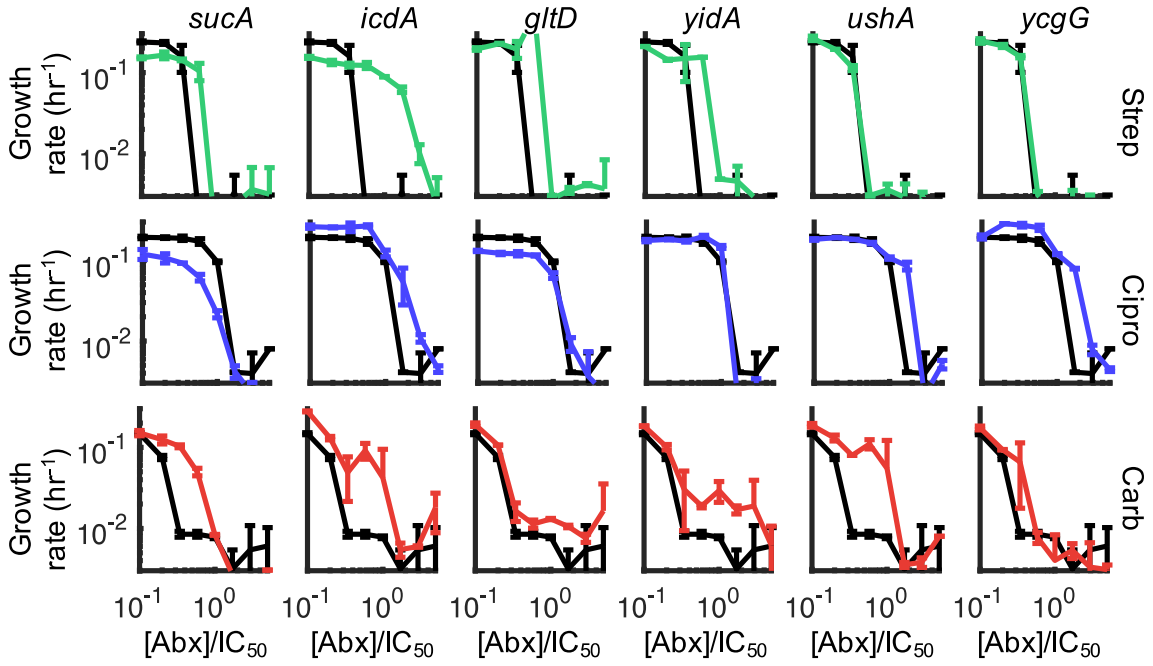


**Fig. S8. Growth inhibition for metabolic mutants,**

Growth rate (y-axis) is plotted as a function of antibiotic concentration normalized by the control strain's $IC_{50}$ value (shown in black). The intact BW25113 carrying pAB191 is used as the WT control. Error bars represent the standard deviations of three biological replicates.

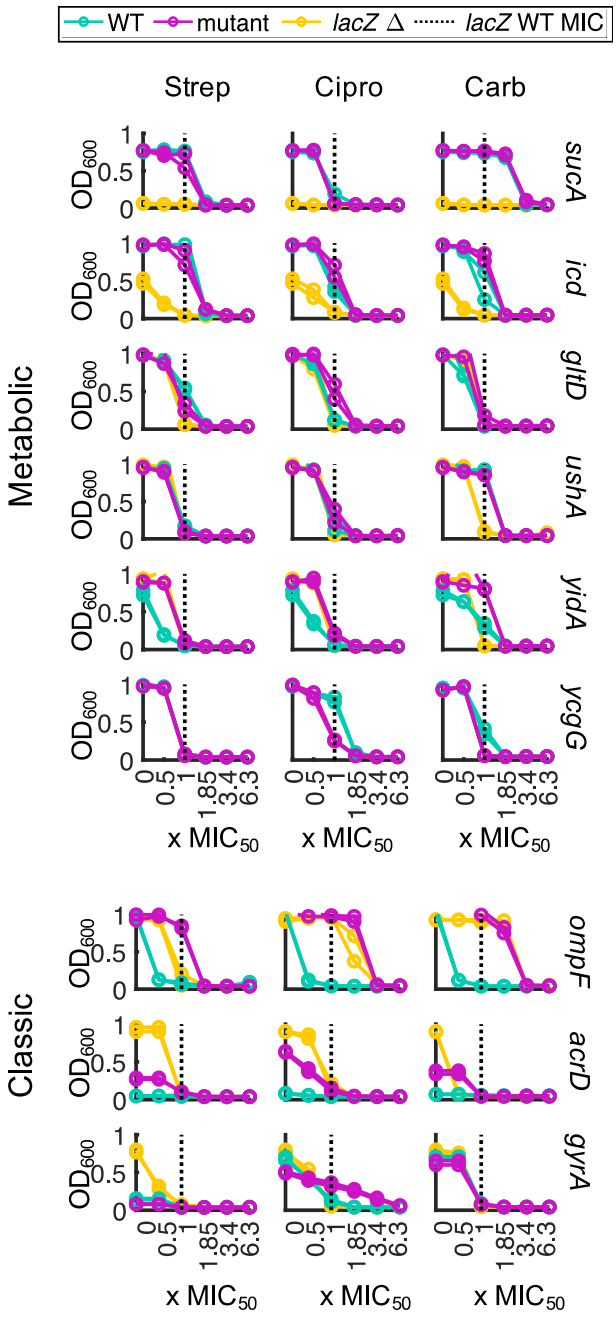


**Fig. S9. MICs for metabolic mutants.**

MICs measured for mutant (green) and WT (yellow) sequences of the same representative subset of genes as in Fig. 4B. The intact BW25113 carrying pAB191 is used as the WT control (vertical dashed black line). Knockout controls, which correspond to each strain carrying pAB191, are shown in pink. Two biological replicates were obtained for each condition; both are plotted in each figure without averaging to demonstrate variability if present.

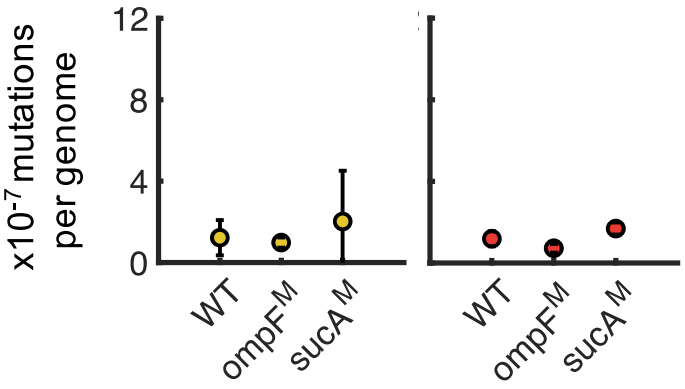


**Fig. S10. Rifampicin mutation rate.**

Mutation rates for the control strain compared to the *ompF* and *sucA* mutant (sucA$^{M}$) strains. Error bars show 95% confidence interval.

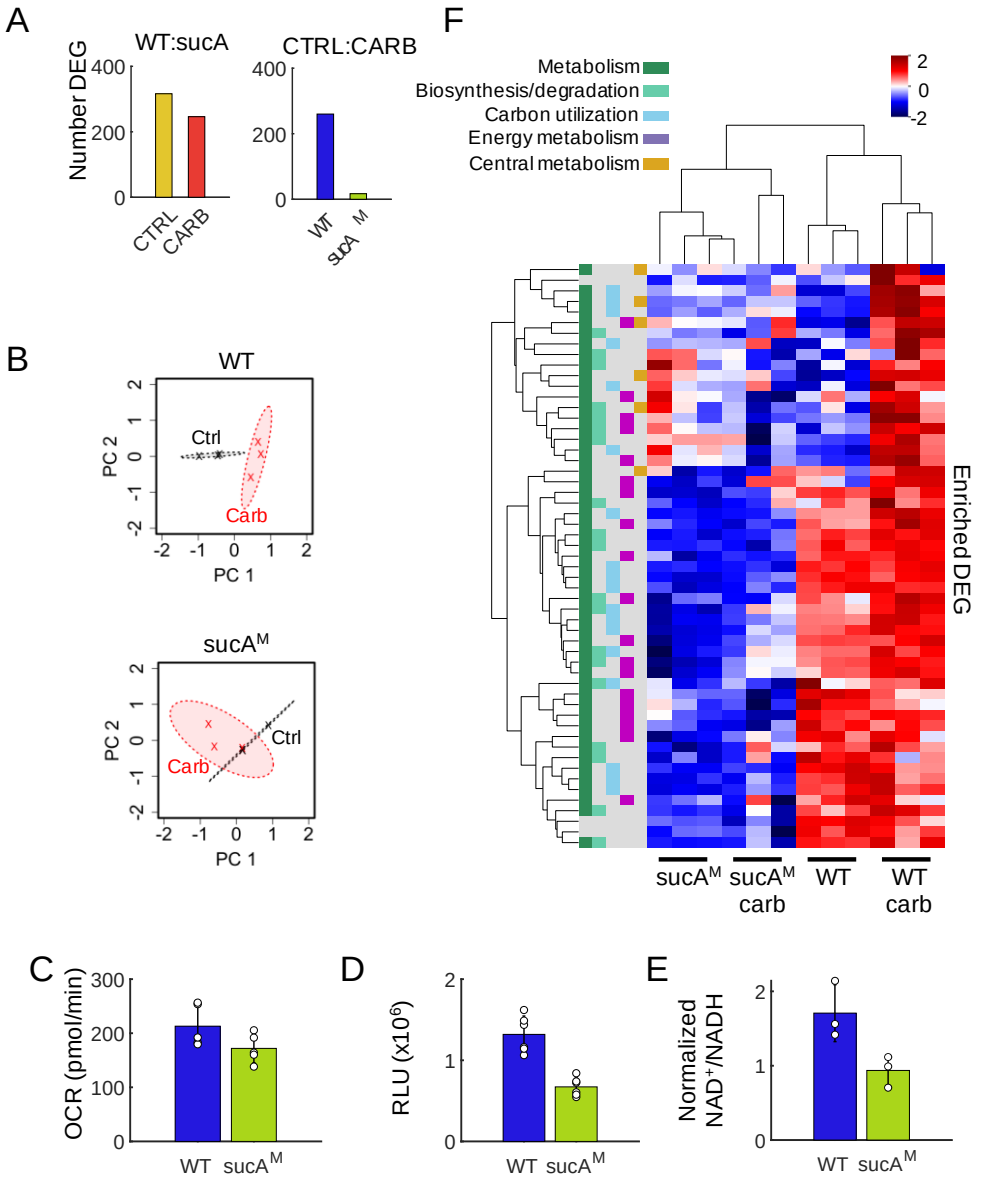


**Fig. S11. Mechanistic validation.**

**(A)** Left: Number of differentially expressed genes between the WT and sucA$^{M}$ in the absence (yellow) and presence (red) of carb treatment. Right: Number of differentially expressed genes between the treated and untreated conditions for WT (blue) and sucA$^{M}$ (green). In all cases when compared to the mutant strain, WT corresponds to BW25113 carrying pAB191. **(B)** Principle component plots for WT (top) and sucA$^{M}$ (bottom) with (red) and without (black) carb treatment. Ellipses represent 1.5 standard deviations. **(C)** Oxygen consumption rates between WT (blue) and sucA$^{M}$ (green) are significantly different (P =0.0077, student two-tailed t-test). **(D)** ATP levels between WT (blue) and sucA$^{M}$ (green) are significantly different (P = 9.3x10$^{-5}$). **(E)** NAD$^{+}$/NADH ratios of WT (blue) and sucA$^{M}$ (green) in response to strep, cipro, or carb. Values were normalized with respect to the untreated control at the same time point. NADH$^{+}$/NADH ratios are statistically different for sucA$^{M}$ cells after carb treatment (P = 0.03, student two-tailed t-test). Data are normalized to each respective cell strain in the absence of treatment. **(F)** Same data as in Fig. 4C with clustered columns in addition to clustered rows.

**Table S1.**

**(A)** All strains used in this study

| Designation | Description | Genotype | Source |
|---|---|---|---|
| WT | *E. coli* strain BW25113 | F$^-$, *Δ(araD-araB)567, ΔlacZ4787(::*rrnB-3*), λ$^-$, rph-1, Δ(rhaD-rhaB)568, hsdR514* | Lab stock |
| Δ*icd::kan* | *E. coli* strain BW25113 with *icd* knocked out | F$^-$, *Δ(araD-araB)567, ΔlacZ4787(::*rrnB-3*), λ$^-$, Δ(icd724::kan), rph-1, Δ(rhaD-rhaB)568, hsdR514* | Keio collection; JW1122-2 |
| Δ*ushA::kan* | *E. coli* strain BW25113 with *ushA* knocked out | F$^-$, *Δ(araD-araB)567, ΔlacZ4787(::*rrnB-3*), λ$^-$, Δ(ushA763::kan), rph-1, Δ(rhaD-rhaB)568, hsdR514* | Keio collection; JW0469-4 |
| Δ*ompF::kan* | *E. coli* strain BW25113 with *ompF* knocked out | F$^-$, *Δ(araD-araB)567, ΔlacZ4787(::*rrnB-3*), λ$^-$, Δ(ompF746::kan), rph-1, Δ(rhaD-rhaB)568, hsdR514* | Keio collection; JW0912-1 |
| Δ*sucA::kan* | *E. coli* strain BW25113 with *sucA* knocked out | F$^-$, *Δ(araD-araB)567, ΔlacZ4787(::*rrnB-3*), λ$^-$, Δ(sucA775::kan), rph-1, Δ(rhaD-rhaB)568, hsdR514* | Keio collection; JW0715-2 |
| Δ*gltD::kan* | *E. coli* strain BW25113 with *gltD* knocked out | F$^-$, *Δ(araD-araB)567, ΔlacZ4787(::*rrnB-3*), λ$^-$, Δ(gltD742::kan), rph-1, Δ(rhaD-rhaB)568, hsdR514* | Keio collection; JW3180-1 |
| Δ*ycgG::kan* | *E. coli* strain BW25113 with *yccG* knocked out | F$^-$, *Δ(araD-araB)567, ΔlacZ4787(::*rrnB-3*), λ$^-$, Δ(ycgG757::kan), rph-1, Δ(rhaD-rhaB)568, hsdR514* | Keio collection; JW5174-1 |
| Δ*acrD::kan* | *E. coli* strain BW25113 with *acrD* knocked out and kanamycin resistance removed | F$^-$, *Δ(araD-araB)567, ΔlacZ4787(::*rrnB-3*), λ$^-$, Δ(acrD790), rph-1, Δ(rhaD-rhaB)568, hsdR514* | Keio collection; JW2454-1 |
| Δ*icd* | *E. coli* strain BW25113 with *icd* knocked out and kanamycin resistance removed | F$^-$, *Δ(araD-araB)567, ΔlacZ4787(::*rrnB-3*), λ$^-$, Δ(icd724), rph-1, Δ(rhaD-rhaB)568, hsdR514* | Generated in this study |
| Δ*ushA* | *E. coli* strain BW25113 with *ushA* knocked out and kanamycin resistance | F$^-$, *Δ(araD-araB)567, ΔlacZ4787(::*rrnB-3*), λ$^-$, Δ(ushA763),* | Generated in this study |

| | | | |
|---|---|---|---|
| | removed | *rph-1, Δ(rhaD-rhaB)568, hsdR514* | |
| Δ*ompF* | *E. coli* strain BW25113 with *ompF* knocked out and kanamycin resistance removed | F$^-$, *Δ(araD-araB)567, ΔlacZ4787(::*rrnB-3*), λ$^-$, Δ(ompF746), rph-1, Δ(rhaD-rhaB)568, hsdR514* | Generated in this study |
| Δ*sucA* | *E. coli* strain BW25113 with *sucA* knocked out and kanamycin resistance removed | F$^-$, *Δ(araD-araB)567, ΔlacZ4787(::*rrnB-3*), λ$^-$, Δ(sucA775), rph-1, Δ(rhaD-rhaB)568, hsdR514* | Generated in this study |
| Δ*gltD* | *E. coli* strain BW25113 with *gltD* knocked out and kanamycin resistance removed | F$^-$, *Δ(araD-araB)567, ΔlacZ4787(::*rrnB-3*), λ$^-$, Δ(gltD742), rph-1, Δ(rhaD-rhaB)568, hsdR514* | Generated in this study |
| Δ*ycgG* | *E. coli* strain BW25113 with *yccG* knocked out and kanamycin resistance removed | F$^-$, *Δ(araD-araB)567, ΔlacZ4787(::*rrnB-3*), λ$^-$, Δ(ycgG757), rph-1, Δ(rhaD-rhaB)568, hsdR514* | Generated in this study |
| Δ*acrD* | *E. coli* strain BW25113 with *acrD* knocked out and kanamycin resistance removed | F$^-$, *Δ(araD-araB)567, ΔlacZ4787(::*rrnB-3*), λ$^-$, Δ(acrD790), rph-1, Δ(rhaD-rhaB)568, hsdR514* | Generated in this study |

**(B)** All plasmids used in this study. $Cm^R$ and $amp^R$ denotes chloramphenicol and ampicillin resistance, respectively.

| Plasmid | Description | Resistance |
|---|---|---|
| pAB191 | p15A ori; proD promoter driving lacZ | $cm^R$ |
| pCP20 | pSC101(ts) ori; $\lambda_{PR}$ promoter driving flp recombinase | $cm^R$, $amp^R$ |
| pAB01a | p15A ori; proD promoter driving *icdA*$^+$ | $cm^R$ |
| pAB01b | p15A ori; proD promoter driving *icdA*-1 | $cm^R$ |
| pAB02a | p15A ori; proD promoter driving *sucA*$^+$ | $cm^R$ |
| pAB02b | p15A ori; proD promoter driving *sucA-1* | $cm^R$ |
| pAB04a | p15A ori; proD promoter driving *ushA*$^+$ | $cm^R$ |
| pAB04b | p15A ori; proD promoter driving *ushA*-1 | $cm^R$ |
| pAB05a | p15A ori; proD promoter driving *yidA*$^+$ | $cm^R$ |
| pAB05b | p15A ori; proD promoter driving *yidA*-1 | $cm^R$ |
| pAB07a | p15A ori; proD promoter driving *gltD*$^+$ | $cm^R$ |
| pAB07b | p15A ori; proD promoter driving *gltD*-1 | $cm^R$ |
| pAB08a | p15A ori; proD promoter driving *acrD*$^+$ | $cm^R$ |
| pAB08b | p15A ori; proD promoter driving *acrD*-1 | $cm^R$ |
| pAB09a | p15A ori; proD promoter driving *ompF*$^+$ | $cm^R$ |
| pAB09b | p15A ori; proD promoter driving *ompF*-1 | $cm^R$ |
| pAB09a | p15A ori; proD promoter driving *gyrA*$^+$ | $cm^R$ |
| pAB09b | p15A ori; proD promoter driving *gyrA*-1 | $cm^R$ |

| | | |
|---|---|---|
| pAB09b | p15A ori; proD promoter driving *yccG*-1 | $cm^R$ |

**(C)** Primer sequences.

| | | |
|---|---|---|
| ACCTGCAGGTGCAGUaaggaggaaaaaaaaatgcagaacagcgctttga | Fwd | Amplifies the 5' end of sucA |
| AGTGCCGTTAATTAAGUcttttattcgacgttcagcgcgt | Rev | Amplifies the 3' end of sucA |
| ATGCTGGCGATTGCGUggtggcagagtggcgtccg | Fwd | Amplifies the middle of sucA mutant |
| ACGCAATCGCCAGCATcc | Rev | Amplifies the middle of sucA mutant |
| ACCTGCAGGTGCAGUaaggaggaaaaaaaaatggctattaaactcattgctatcga | Fwd | Amplifies the 5' end of yidA, includes SD8 RBS |
| AGTGCCGTTAATTAAGUcttttaattcagcacatacttctcaatagc | Rev | Amplifies the 3' end of yidA |
| ACCTGCAGGTGCAGUaaggaggaaaaaaaaatggctattaaactcattgctatcgatatggatggccccccttctgctgcccgatc | Fwd | Amplifies the 5' end of yidA mutant, includes SD8 RBS |
| ACCTGCAGGTGCAGUaaggaggaaaaaaaaatggcgaatttctttattgatcg | Fwd | Amplifies the 5' end of acrD, includes SD8 RBS |
| AGTGCCGTTAATTAAGUagcttttattccgggcgcggcttcagc | Rev | Amplifies the 3' end of acrD |
| ACCTGCAGGTGCAGUaaggaggaaaaaaaaatgacgaatttctttattgatcgcccca | Fwd | Amplifies the 5' end of acrD mutant, includes SD8 RBS |
| AGGCATCTGGATUgtgcagg | Fwd | Amplifies the middle of ushA mutant |
| AATCCAGATGCCUttttgttgatctggtttgcatgg | Rev | Amplifies the middle of ushA mutant |
| ACCTGCAGGTGCAGUaaggaggaaaaaaaaatgagtcagaatgtttatcaatttatcgac | Fwd | Amplifies the 5' end of gltD, includes SD8 RBS |
| AGTGCCGTTAATTAAGUcttttaaacttccagccagttcataatac | Rev | Amplifies the 3' end of gltD |
| AGATAAAGCGTUcgagatgggc | Fwd | Amplifies the middle of gltD mutant |
| AACGCTTTATCUttgatatagcgctcaatgttgcc | Rev | Amplifies the middle of gltD mutant |
| ACCTGCAGGTGCAGUaaggaggaaaaaaaaatgttgtacgataaatcccttgagag | Fwd | Amplifies the 5' end of gltB, includes SD8 RBS |
| AGTGCCGTTAATTAAGUcttttactgcgcctgcacg | Rev | Amplifies the 3' end of gltB |
| ACCGAGCATGUgccgcataccggctctcagc | Fwd | Amplifies the middle of gltB mutant |
| ACATGCTCGGUgataagacca | Rev | Amplifies the middle of gltB mutant |
| ACCTGCAGGTGCAGUaaggaggaaaaaaaaatgagcgacctgcgagag | Fwd | Amplifies the 5' end of gyrA, includes SD8 RBS |

| | | |
|---|---|---|
| AGTGCCGTTAATTAAGUcttttattcttcttctggctcgtcg | Rev | Amplifies the 3' end of gyrA |
| ATGGTGACTUggcggtctatgacacgatcg | Fwd | Amplifies the middle of gyrA mutant |
| AAGTCACCAUggggatggtatttaccgat | Rev | Amplifies the middle of gyrA mutant |
| AACCGTAACCTAUgacttcgagc | Fwd | Amplifies the middle of icdA mutant |
| ATAGGTTACGGTUttggcgttgattgcgccttccatacc | Rev | Amplifies the middle of icdA mutant |
| ATCGTTGGTGCTUaGCTTATggtgcagctgaccgtacc | Fwd | Amplifies the middle of ompF mutant |
| AAGCACCAACGAUaccaaagc | Rev | Amplifies the middle of ompF mutant |
| ACTTAATTAACGGCACTC | Fwd | Linearizes pAB191 for gibson assembly |
| TTTTTTTTCCTCCTTACTGC | Rev | Linearizes pAB191 for gibson assembly |
| gcagtaaggaggaaaaaaaaATGATGAAGCGCAATATTC | Fwd | Amplifies the 5' end of ompF |
| aggagtgccgttaattaagtCTTTTAGAACTGGTAAACGATAC | Rev | Amplifies the 3' end of ompF |
| aggagtgccgttaattaagtCTTTTACTGCCAGCTCAC | Fwd | Amplifies the 5' end of ushA |
| gcagtaaggaggaaaaaaaaATGCGCAATACACTCATAC | Rev | Amplifies the 3' end of ushA |
| gcagtaaggaggaaaaaaaaATGGAAAGTAAAGTAGTTGTTC | Fwd | Amplifies the 5' end of icdA |
| aggagtgccgttaattaagtCTTTTACATGTTTTCGATGATC | Rev | Amplifies the 3' end of icdA |
| gcagtaaggaggaaaaaaaaATGCGCAATACACTCATAC | Fwd | Amplifies the 5' end of ycgG |
| AGGAGTGCCGTTAATTAAGTCTTTCACTCAACCACAAC | Rev | Amplifies the 3' end of ycgG |

**Table S2.**

**(A)** $MIC_{50}$ values.

| | MOPS EZ Rich | MOPS Minimal + 0.04% Glucose | Catalog # |
|---|---|---|---|
| **Strep (μg/mL)** | 1.4 | 0.4 | Sigma, #S6501 |
| **Cipro (μg/mL)** | 0.01 | 0.01 | Sigma, #17850 |
| **Carb (μg/mL)** | 12.0 | 3.6 | Sigma, #C1389 |

**(B)** Classic evolution.

| **DATE** | 4/29/19 | 4/30/19 | 5/1/19 | 5/2/19 | 5/3/19 | 5/4/19 | 5/5/19 | 5/6/19 | 5/7/19 | 5/8/19 | 5/9/19 |
|---|---|---|---|---|---|---|---|---|---|---|---|
| **Temperature** | 37 | 37 | 37 | 37 | 37 | 37 | 37 | 37 | 37 | 37 | 37 |
| **Day** | 0 | 1 | 2 | 3 | 4 | 5 | 6 | 7 | 8 | 9 | 10 |
| **Drug multiple*** | 0.085 | 0.16 | 0.29 | 0.54 | 1.00 | 1.85 | 3.42 | 6.33 | 11.71 | 21.67 | 40.09 |
| **Strep (μg/mL)** | 0.1 | 0.2 | 0.4 | 0.8 | 1.4 | 2.6 | 4.8 | 8.9 | 16.4 | 30.3 | 56.1 |
| **Cipro (μg/mL)** | 0.0 | 0.0 | 0.0 | 0.0 | 0.0 | 0.0 | 0.0 | 0.1 | 0.1 | 0.2 | 0.4 |
| **Carb (μg/mL)** | 1.0 | 1.9 | 3.5 | 6.5 | 12.0 | 22.2 | 41.1 | 76.0 | 140.6 | 260.0 | 481.1 |

* Drug multiple corresponds to a multiplication factor for each antibiotic $MIC_{50}$ value

**(C)** Metabolic evolution: rich media.

| **DATE** | 4/29/19 | 4/30/19 | 5/1/19 | 5/2/19 | 5/3/19 | 5/4/19 | 5/5/19 | 5/6/19 | 5/7/19 | 5/8/19 | 5/9/19 |
|---|---|---|---|---|---|---|---|---|---|---|---|
| **Temperature** | 20 | 21 | 22 | 23 | 24 | 25 | 26 | 27 | 28 | 29 | 30 |
| **Day** | 0 | 1 | 2 | 3 | 4 | 5 | 6 | 7 | 8 | 9 | 10 |
| **Drug multiple*** | 40.09 | 40.09 | 40.09 | 40.09 | 40.09 | 40.09 | 40.09 | 40.09 | 40.09 | 40.09 | 40.09 |
| **Strep (μg/mL)** | 56.1 | 56.1 | 56.1 | 56.1 | 56.1 | 56.1 | 56.1 | 56.1 | 56.1 | 56.1 | 56.1 |
| **Cipro (μg/mL)** | 0.4 | 0.4 | 0.4 | 0.4 | 0.4 | 0.4 | 0.4 | 0.4 | 0.4 | 0.4 | 0.4 |
| **Carb (μg/mL)** | 481.1 | 481.1 | 481.1 | 481.1 | 481.1 | 481.1 | 481.1 | 481.1 | 481.1 | 481.1 | 481.1 |

* Drug multiple corresponds to a multiplication factor for each antibiotic $MIC_{50}$ value

**(D)** Metabolic evolution: minimal media.

| **DATE** | 4/29/19 | 4/30/19 | 5/1/19 | 5/2/19 | 5/3/19 | 5/4/19 | 5/5/19 | 5/6/19 | 5/7/19 | 5/8/19 | 5/9/19 |
|---|---|---|---|---|---|---|---|---|---|---|---|
| **Temperature** | 20 | 21 | 22 | 23 | 24 | 25 | 26 | 27 | 28 | 29 | 30 |
| **Day** | 0 | 1 | 2 | 3 | 4 | 5 | 6 | 7 | 8 | 9 | 10 |

| | | | | | | | | | | | |
|---|---|---|---|---|---|---|---|---|---|---|---|
| **Drug multiple*** | 40.09 | 40.09 | 40.09 | 40.09 | 40.09 | 40.09 | 40.09 | 40.09 | 40.09 | 40.09 | 40.09 |
| **Strep (μg/mL)** | 16.0 | 16.0 | 16.0 | 16.0 | 16.0 | 16.0 | 16.0 | 16.0 | 16.0 | 16.0 | 16.0 |
| **Cipro (μg/mL)** | 0.4 | 0.4 | 0.4 | 0.4 | 0.4 | 0.4 | 0.4 | 0.4 | 0.4 | 0.4 | 0.4 |
| **Carb (μg/mL)** | 144.3 | 144.3 | 144.3 | 144.3 | 144.3 | 144.3 | 144.3 | 144.3 | 144.3 | 144.3 | 144.3 |

* Drug multiple corresponds to a multiplication factor for each antibiotic $MIC_{50}$ value

## Captions for Tables S3 to S15

### Additional Data Table S3 (separate file)

Sequencing maps for classic and metabolic evolutions. Sheet one has sequencing maps for the main classic and metabolic evolutions. Sheet two has the sequencing map for the static metabolic evolution.

### Additional Data Table S4 (separate file)

Sequencing results for classic evolution. Sheet one has master data. Sheet two has WT genotype for two replicates. In all subsequent results, tabulations exclude mutations that appeared in the WT strain (*dicC* and *rbsR*).

### Additional Data Table S5 (separate file)

Classic evolution sequencing with KEGG classifications. KEGG and BRITE hierarchy classifications included for the classic evolution sequencing results. Sheet one lists all genes by sample group, and sheet two lists all KEGG functional groups with each associated gene.

### Additional Data Table S6 (separate file)

Sequencing results for metabolic evolution. Column 'evol_exp' designates rich (2_2M) or minimal media (2_1M).

### Additional Data Table S7 (separate file)

Sequencing results for metabolic evolution with static temperature. Sheet one contains master data. Sheet two contains the unique genes for each treatment group.

### Additional Data Table S8 (separate file)

Gene ontology (GO) enrichment for biological processes results. Gene list for GO enrichment from classical evolution. First sheet has data used in Fig. 3B-C. Gray shading indicates rows used for plotting. Sheet two has the list of genes from the metabolic evolution used for GO enrichment and sheet three has the list of genes from the classic evolution used for GO enrichment.

### Additional Data Table S9 (separate file)

Comprehensive list of all NCBI pathogens used in the comparative analysis.

### Additional Data Table S10 (separate file)

Comparative analysis for top genes with >= 1 hit in NCBI pathogen list. Table includes gene name, mutation, number in clinical isolates, number in total isolates, P-value, and corrected P-value. Yellow rows highlight those used for subsequent validation experiments.

**Additional Data Table S11 (separate file)**

Metabolic and canonical gene co-occurrence likelihood. Number of strains that had a mutation in canonical-canonical, metabolic-metabolic, or one of each, was tabulated. Fisher's exact test was used to calculate likelihood of co-occurring mutations.

**Additional Data Table S12 (separate file)**

Raw gene count output from FeatureCounts for each of the 12 samples.

**Additional Data Table S13 (separate file)**

Differential gene expression for pair-wise sample comparison. Log-2 transformed and TMM-normalized CPM for WT and sucA$^{M}$ cells with and without treatment. Differential expression was determined between treated and untreated conditions for each strain-type.

**Additional Data Table S14 (separate file)**

GO enrichment for treated WT compared to sucA$^{M}$. Sheet one contains the corresponding list of genes in the order they were clustered (Fig. 4C). Sheet two contains GO pathway enrichment for all differentially expressed genes between carb-treated WT and sucA$^{M}$.

**Additional Data Table S15 (separate file)**

Gene tabulation across conditions. Sheet contains representative metabolic and canonical mutations along with the conditions in which they occurred; closely related genes are included (e.g., *sucA* and *satP*). Sheet two contains the number of unique genes identified from each condition, along with the overlap between conditions. UN is untreated control.

**References and Notes**


1. A. Giedraitienė, A. Vitkauskienė, R. Naginienė, A. Pavilonis, Antibiotic resistance mechanisms of clinically important bacteria. *Medicina (Kaunas)* **47**, 137–146 (2011). Medline

2. B. A. Espedido, I. B. Gosbell, Chromosomal mutations involved in antibiotic resistance in Staphylococcus aureus. *Front. Biosci. (Schol. Ed.)* **4**, 900–915 (2012). Medline

3. J. H. Yang, S. C. Bening, J. J. Collins, Antibiotic efficacy-context matters. *Curr. Opin. Microbiol.* **39**, 73–80 (2017). doi:10.1016/j.mib.2017.09.002 Medline

4. J. M. Stokes, A. J. Lopatkin, M. A. Lobritz, J. J. Collins, Bacterial metabolism and antibiotic efficacy. *Cell Metab.* **30**, 251–259 (2019). 10.1016/j.cmet.2019.06.009 Medline

5. D. J. Dwyer, P. A. Belenky, J. H. Yang, I. C. MacDonald, J. D. Martell, N. Takahashi, C. T. Y. Chan, M. A. Lobritz, D. Braff, E. G. Schwarz, J. D. Ye, M. Pati, M. Vercruysse, P. S. Ralifo, K. R. Allison, A. S. Khalil, A. Y. Ting, G. C. Walker, J. J. Collins, Antibiotics induce redox-related physiological alterations as part of their lethality. *Proc. Natl. Acad. Sci. U.S.A.* **111**, E2100–E2109 (2014). doi:10.1073/pnas.1401876111 Medline

6. G. I. Lang, M. M. Desai, The spectrum of adaptive mutations in experimental evolution. *Genomics* **104** (6 Pt A), 412–416 (2014). doi:10.1016/j.ygeno.2014.09.011 Medline

7. P. Charusanti, N. L. Fong, H. Nagarajan, A. R. Pereira, H. J. Li, E. A. Abate, Y. Su, W. H. Gerwick, B. O. Palsson, Exploiting adaptive laboratory evolution of *Streptomyces clavuligerus* for antibiotic discovery and overproduction. *PLOS ONE* **7**, e33727 (2012). doi:10.1371/journal.pone.0033727 Medline

8. M. Rodriguez de Evgrafov, H. Gumpert, C. Munck, T. T. Thomsen, M. O. A. Sommer, Collateral resistance and sensitivity modulate evolution of high-level resistance to drug combination treatment in *Staphylococcus aureus*. *Mol. Biol. Evol.* **32**, 1175–1185 (2015). doi:10.1093/molbev/msv006 Medline

9. E. Toprak, A. Veres, J.-B. Michel, R. Chait, D. L. Hartl, R. Kishony, Evolutionary paths to antibiotic resistance under dynamically sustained drug selection. *Nat. Genet.* **44**, 101–105 (2011). doi:10.1038/ng.1034 Medline

10. S. Suzuki, T. Horinouchi, C. Furusawa, Prediction of antibiotic resistance by gene expression profiles. *Nat. Commun.* **5**, 5792 (2014). doi:10.1038/ncomms6792 Medline

11. L. J. Jahn, C. Munck, M. M. H. Ellabaan, M. O. A. Sommer, Adaptive laboratory evolution of antibiotic resistance using different selection regimes lead to similar phenotypes and genotypes. *Front. Microbiol.* **8**, 816 (2017). doi:10.3389/fmicb.2017.00816 Medline

12. J. R. Dettman, N. Rodrigue, A. H. Melnyk, A. Wong, S. F. Bailey, R. Kassen, Evolutionary insight from whole-genome sequencing of experimentally evolved microbes. *Mol. Ecol.* **21**, 2058–2077 (2012). doi:10.1111/j.1365-294X.2012.05484.x Medline

13. M. F. Schenk, J. A. G. M. de Visser, Predicting the evolution of antibiotic resistance. *BMC Biol.* **11**, 14 (2013). doi:10.1186/1741-7007-11-14 Medline

14. A. Couce, A. Rodríguez-Rojas, J. Blázquez, Bypass of genetic constraints during mutator evolution to antibiotic resistance. *Proc. Biol. Sci.* **282**, 20142698 (2015).

doi:10.1098/rspb.2014.2698 Medline

15. J. F. Matias Rodrigues, A. Wagner, Evolutionary plasticity and innovations in complex metabolic reaction networks. *PLOS Comput. Biol.* **5**, e1000613 (2009). doi:10.1371/journal.pcbi.1000613 Medline

16. T. Leinonen, R. J. S. McCairns, G. Herczeg, J. Merilä, Multiple evolutionary pathways to decreased lateral plate coverage in freshwater threespine sticklebacks. *Evolution* **66**, 3866–3875 (2012). Medline

17. A. Wilm, P. P. K. Aw, D. Bertrand, G. H. T. Yeo, S. H. Ong, C. H. Wong, C. C. Khor, R. Petric, M. L. Hibberd, N. Nagarajan, LoFreq: A sequence-quality aware, ultra-sensitive variant caller for uncovering cell-population heterogeneity from high-throughput sequencing datasets. *Nucleic Acids Res.* **40**, 11189–11201 (2012). doi:10.1093/nar/gks918 Medline

18. J. L. Martinez, F. Baquero, Mutation frequencies and antibiotic resistance. *Antimicrob. Agents Chemother.* **44**, 1771–1777 (2000). doi:10.1128/AAC.44.7.1771-1777.2000 Medline

19. S. F. Levy, J. R. Blundell, S. Venkataram, D. A. Petrov, D. S. Fisher, G. Sherlock, Quantitative evolutionary dynamics using high-resolution lineage tracking. *Nature* **519**, 181–186 (2015). doi:10.1038/nature14279 Medline

20. I. Levin-Reisman, I. Ronin, O. Gefen, I. Braniss, N. Shoresh, N. Q. Balaban, Antibiotic tolerance facilitates the evolution of resistance. *Science* **355**, 826–830 (2017). doi:10.1126/science.aaj2191 Medline

21. Materials and methods are available as supplementary materials.

22. K. McElroy, T. Thomas, F. Luciani, Deep sequencing of evolving pathogen populations: Applications, errors, and bioinformatic solutions. *Microb. Inform. Exp.* **4**, 1 (2014). doi:10.1186/2042-5783-4-1 Medline

23. A. Wong, N. Rodrigue, R. Kassen, Genomics of adaptation during experimental evolution of the opportunistic pathogen *Pseudomonas aeruginosa*. *PLOS Genet.* **8**, e1002928 (2012). doi:10.1371/journal.pgen.1002928 Medline

24. R. E. Lenski, M. Travisano, Dynamics of adaptation and diversification: A 10,000-generation experiment with bacterial populations. *Proc. Natl. Acad. Sci. U.S.A.* **91**, 6808–6814 (1994). doi:10.1073/pnas.91.15.6808 Medline

25. T. Oz, A. Guvenek, S. Yildiz, E. Karaboga, Y. T. Tamer, N. Mumcuyan, V. B. Ozan, G. H. Senturk, M. Cokol, P. Yeh, E. Toprak, Strength of selection pressure is an important parameter contributing to the complexity of antibiotic resistance evolution. *Mol. Biol. Evol.* **31**, 2387–2401 (2014). doi:10.1093/molbev/msu191 Medline

26. A. H. Melnyk, A. Wong, R. Kassen, The fitness costs of antibiotic resistance mutations. *Evol. Appl.* **8**, 273–283 (2015). doi:10.1111/eva.12196 Medline

27. H. H. Lee, M. N. Molla, C. R. Cantor, J. J. Collins, Bacterial charity work leads to population-wide resistance. *Nature* **467**, 82–85 (2010). doi:10.1038/nature09354 Medline

28. B. J. Walker, T. Abeel, T. Shea, M. Priest, A. Abouelliel, S. Sakthikumar, C. A. Cuomo, Q.

Zeng, J. Wortman, S. K. Young, A. M. Earl, Pilon: An integrated tool for comprehensive microbial variant detection and genome assembly improvement. *PLOS ONE* **9**, e112963 (2014). doi:10.1371/journal.pone.0112963 Medline

29. D. I. Andersson, D. Hughes, Persistence of antibiotic resistance in bacterial populations. *FEMS Microbiol. Rev.* **35**, 901–911 (2011). doi:10.1111/j.1574-6976.2011.00289.x Medline

30. L. Pinto, C. Torres, C. Gil, J. D. Nunes-Miranda, H. M. Santos, V. Borges, J. P. Gomes, C. Silva, L. Vieira, J. E. Pereira, P. Poeta, G. Igrejas, Multiomics assessment of gene expression in a clinical strain of CTX-M-15-producing ST131 *Escherichia coli*. *Front. Microbiol.* **10**, 831 (2019). doi:10.3389/fmicb.2019.00831 Medline

31. A. N. Woodmansee, J. A. Imlay, Reduced flavins promote oxidative DNA damage in non-respiring *Escherichia coli* by delivering electrons to intracellular free iron. *J. Biol. Chem.* **277**, 34055–34066 (2002). doi:10.1074/jbc.M203977200 Medline

32. D.-E. Chang, D. J. Smalley, T. Conway, Gene expression profiling of *Escherichia coli* growth transitions: An expanded stringent response model. *Mol. Microbiol.* **45**, 289–306 (2002). doi:10.1046/j.1365-2958.2002.03001.x Medline

33. I. Levin-Reisman, A. Brauner, I. Ronin, N. Q. Balaban, Epistasis between antibiotic tolerance, persistence, and resistance mutations. *Proc. Natl. Acad. Sci. U.S.A.* **116**, 14734–14739 (2019). doi:10.1073/pnas.1906169116 Medline

34. I. Levin-Reisman, O. Fridman, N. Q. Balaban, ScanLag: High-throughput quantification of colony growth and lag time. *J. Vis. Exp.* (89): (2014). doi:10.3791/51456 Medline

35. M. Oram, L. M. Fisher, 4-Quinolone resistance mutations in the DNA gyrase of *Escherichia coli* clinical isolates identified by using the polymerase chain reaction. *Antimicrob. Agents Chemother.* **35**, 387–389 (1991). doi:10.1128/AAC.35.2.387 Medline

36. H. Yoshida, M. Bogaki, M. Nakamura, S. Nakamura, Quinolone resistance-determining region in the DNA gyrase gyrA gene of *Escherichia coli*. *Antimicrob. Agents Chemother.* **34**, 1271–1272 (1990). doi:10.1128/AAC.34.6.1271 Medline

37. J. Vila, J. Ruiz, F. Marco, A. Barcelo, P. Goñi, E. Giralt, T. Jimenez de Anta, Association between double mutation in gyrA gene of ciprofloxacin-resistant clinical isolates of *Escherichia coli* and MICs. *Antimicrob. Agents Chemother.* **38**, 2477–2479 (1994). doi:10.1128/AAC.38.10.2477 Medline

38. M. A. Kohanski, D. J. Dwyer, B. Hayete, C. A. Lawrence, J. J. Collins, A common mechanism of cellular death induced by bactericidal antibiotics. *Cell* **130**, 797–810 (2007). doi:10.1016/j.cell.2007.06.049 Medline

39. J. M. A. Blair, M. A. Webber, A. J. Baylay, D. O. Ogbolu, L. J. V. Piddock, Molecular mechanisms of antibiotic resistance. *Nat. Rev. Microbiol.* **13**, 42–51 (2015). doi:10.1038/nrmicro3380 Medline

40. N. Woodford, M. J. Ellington, The emergence of antibiotic resistance by mutation. *Clin. Microbiol. Infect.* **13**, 5–18 (2007). doi:10.1111/j.1469-0691.2006.01492.x Medline

41. M. Zampieri, T. Enke, V. Chubukov, V. Ricci, L. Piddock, U. Sauer, Metabolic constraints on the evolution of antibiotic resistance. *Mol. Syst. Biol.* **13**, 917 (2017).

doi:10.15252/msb.20167028 Medline

42. M. Zampieri, M. Zimmermann, M. Claassen, U. Sauer, Nontargeted metabolomics reveals the multilevel response to antibiotic perturbations. *Cell Rep.* **19**, 1214–1228 (2017). doi:10.1016/j.celrep.2017.04.002 Medline

43. A. J. Lopatkin, S. C. Bening, A. L. Manson, J. M. Stokes, M. A. Kohanski, A. H. Badran, A. M. Earl, N. J. Cheney, J. H. Yang, J. J. Collins, Mathematical model code for: Clinically relevant mutations in core metabolic genes confer antibiotic resistance (2020); https://doi.org/10.5281/zenodo.4323054.

44. G. I. Lang, D. Botstein, M. M. Desai, Genetic variation and the fate of beneficial mutations in asexual populations. *Genetics* **188**, 647–661 (2011). doi:10.1534/genetics.111.128942 Medline

45. M. M. Desai, D. S. Fisher, Beneficial mutation selection balance and the effect of linkage on positive selection. *Genetics* **176**, 1759–1798 (2007). doi:10.1534/genetics.106.067678 Medline

46. N. Gompel, B. Prud'homme, The causes of repeated genetic evolution. *Dev. Biol.* **332**, 36–47 (2009). doi:10.1016/j.ydbio.2009.04.040 Medline

47. A. J. Lopatkin, S. Huang, R. P. Smith, J. K. Srimani, T. A. Sysoeva, S. Bewick, D. K. Karig, L. You, Antibiotics as a selective driver for conjugation dynamics. *Nat. Microbiol.* **1**, 16044 (2016). doi:10.1038/nmicrobiol.2016.44 Medline

48. A. J. Lopatkin, H. R. Meredith, J. K. Srimani, C. Pfeiffer, R. Durrett, L. You, Persistence and reversal of plasmid-mediated antibiotic resistance. *Nat. Commun.* **8**, 1689 (2017). doi:10.1038/s41467-017-01532-1 Medline

49. H. Li, R. Durbin, Fast and accurate short read alignment with Burrows-Wheeler transform. *Bioinformatics* **25**, 1754–1760 (2009). doi:10.1093/bioinformatics/btp324 Medline

50. D. Zhang, J. E. Gomez, J.-Y. Chien, N. Haseley, C. A. Desjardins, A. M. Earl, P.-R. Hsueh, D. T. Hung, Genomic analysis of the evolution of fluoroquinolone resistance in *Mycobacterium tuberculosis* prior to tuberculosis diagnosis. *Antimicrob. Agents Chemother.* **60**, 6600–6608 (2016). doi:10.1128/AAC.00664-16 Medline

51. E. I. Boyle, S. Weng, J. Gollub, H. Jin, D. Botstein, J. M. Cherry, G. Sherlock, GO:TermFinder—Open source software for accessing Gene Ontology information and finding significantly enriched Gene Ontology terms associated with a list of genes. *Bioinformatics* **20**, 3710–3715 (2004). doi:10.1093/bioinformatics/bth456 Medline

52. G. C. Cerqueira, A. M. Earl, C. M. Ernst, Y. H. Grad, J. P. Dekker, M. Feldgarden, S. B. Chapman, J. L. Reis-Cunha, T. P. Shea, S. Young, Q. Zeng, M. L. Delaney, D. Kim, E. M. Peterson, T. F. O'Brien, M. J. Ferraro, D. C. Hooper, S. S. Huang, J. E. Kirby, A. B. Onderdonk, B. W. Birren, D. T. Hung, L. A. Cosimi, J. R. Wortman, C. I. Murphy, W. P. Hanage, Multi-institute analysis of carbapenem resistance reveals remarkable diversity, unexplained mechanisms, and limited clonal outbreaks. *Proc. Natl. Acad. Sci. U.S.A.* **114**, 1135–1140 (2017). doi:10.1073/pnas.1616248114 Medline

53. R. C. Edgar, MUSCLE: Multiple sequence alignment with high accuracy and high throughput. *Nucleic Acids Res.* **32**, 1792–1797 (2004). doi:10.1093/nar/gkh340 Medline

54. M. A. Kohanski, M. A. DePristo, J. J. Collins, Sublethal antibiotic treatment leads to multidrug resistance via radical-induced mutagenesis. *Mol. Cell* **37**, 311–320 (2010). doi:10.1016/j.molcel.2010.01.003 Medline

55. W. A. Rosche, P. L. Foster, Determining mutation rates in bacterial populations. *Methods* **20**, 4–17 (2000). doi:10.1006/meth.1999.0901 Medline

56. A. M. Bolger, M. Lohse, B. Usadel, Trimmomatic: A flexible trimmer for Illumina sequence data. *Bioinformatics* **30**, 2114–2120 (2014). doi:10.1093/bioinformatics/btu170 Medline

57. A. Dobin, C. A. Davis, F. Schlesinger, J. Drenkow, C. Zaleski, S. Jha, P. Batut, M. Chaisson, T. R. Gingeras, STAR: Ultrafast universal RNA-seq aligner. *Bioinformatics* **29**, 15–21 (2013). doi:10.1093/bioinformatics/bts635 Medline

58. Y. Liao, G. K. Smyth, W. Shi, featureCounts: An efficient general purpose program for assigning sequence reads to genomic features. *Bioinformatics* **30**, 923–930 (2014). doi:10.1093/bioinformatics/btt656 Medline

59. M. D. Robinson, D. J. McCarthy, G. K. Smyth, edgeR: A Bioconductor package for differential expression analysis of digital gene expression data. *Bioinformatics* **26**, 139–140 (2010). doi:10.1093/bioinformatics/btp616 Medline